Helical Mode Formed in the Initial Region of a Round Jet by Synthetic jets

A. Muramatsu[1]*

1: Dept. of Aerospace Engineering, Nihon University, Japan

* Correspondent author: muramatsu.akinori@nihon-u.ac.jp

Abstract

Round jets have symmetric and asymmetric modes. In a round jet of natural transition, an axisymmetric mode is typically observed in the initial region of the jet near the nozzle exit, while a helical mode develops downstream of the initial region where the potential core disappears. However, by controlling the jet, asymmetric mode, i.e., helical mode, can be formed near the nozzle. Here, a round nozzle has three holes for the synthetic jets. The three holes are positioned at equal intervals around the circumference of the nozzle. By sequentially driving the three synthetic jets, a helical structure is formed near the nozzle exit of the round jet. The frequency of the synthetic jets is set to the frequency of vortex-ring formation in the natural transition. The results of numerical simulation using OpenFOAM and experimental results, such as, flow visualizations and PIV measurements, are presented for this flow field.

Keyword: *Round jet, Helical structure, Spiral structure, Synthetic jet, Flow control*

1. Introduction

The unstable modes of round jets include an axisymmetric mode (varicose mode), which is related to the formation of vortex rings, and an asymmetric mode (helical mode), which forms spiral structures [1]. In round jets with natural transition, the axisymmetric mode is observed in the initial region of the jet near the nozzle exit, and the helical mode appears downstream of the initial region where the potential core disappears. However, it has been shown that the helical mode can be induced from the nozzle exit by perturbing the jet. For example, Koch et al. (2) demonstrated through experiments by flow visualization that a helical vortex structure can be formed in the initial region of a round jet by driving four loudspeakers with a phase difference. Kiwata et al. [3] showed that both helical mode and symmetric mode jets can be generated by using a coaxial jet.

On the other hand, Tanaka and Muramatsu [4] artificially formed bifurcating flows in the initial region of a round jet by driving the synthetic jets in the same phase. Holes for synthetic jets are located at equal intervals in the circumferential direction on the side wall of a round nozzle. Using this nozzle, numerical simulations were conducted [5] based on the idea that a helical mode could be formed in the initial region of the round jet by driving the synthetic jets in sequence, as in the case of Koch et al. [2]. The results showed that a helical structure could be formed using three or more synthetic jets. In this study, we present the results of numerical simulation and experiments of a jet forming a helical structure near the nozzle exit when three synthetic jets are driven at the frequency of vortex ring formation in the natural transition of the jet.

2. Experimental Apparatus and Conditions

Schematic views of a round nozzle and experimental apparatus used in experiments are shown in Figs. 1 and 2. As illustrated in Fig. 1, the round nozzle has an exit diameter D_0 of 12 mm, an area contraction ratio of 30.3, and three holes of 2 mm in diameter spaced equally in the circumferential direction to form three synthetic jets. These holes are connected through vinyl tubes to three speaker boxes, each containing an acoustic loudspeaker (Fostex, FE103). Each loudspeaker is driven by a sinusoidal wave generated by a three-output signal generator (Walffront, FY8300), and three synthetic jets are produced from the holes.

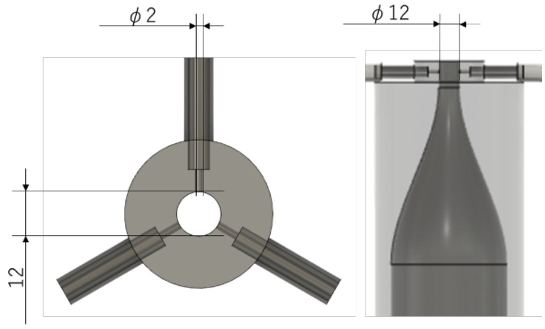

Fig. 1 A round nozzle with three holes.

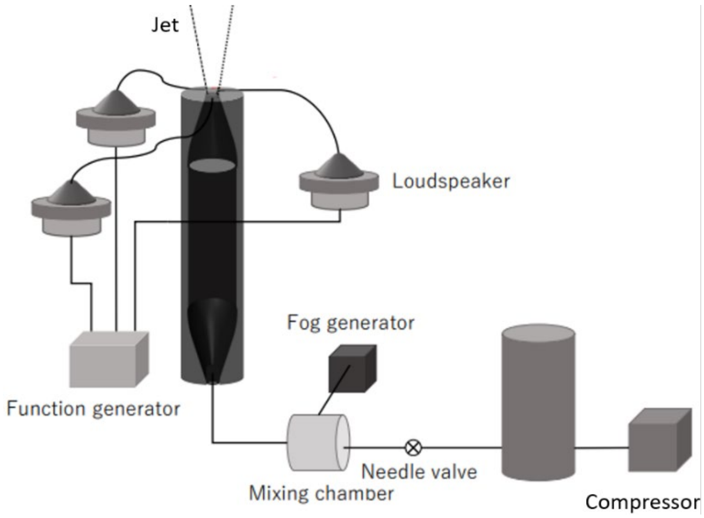

Fig. 2 Experimental apparatus.

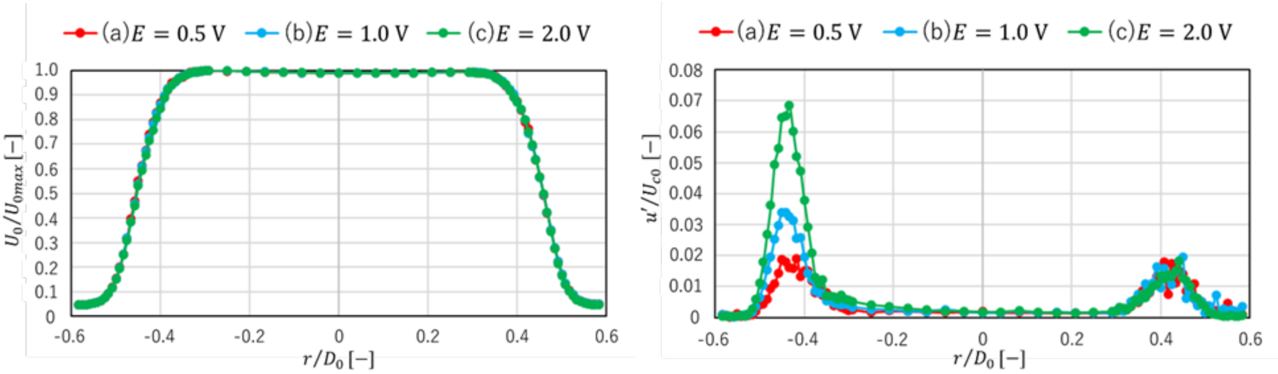

(a) Mean velocity profiles (b) Turbulent intensity profiles

Fig. 3 Profiles of mean velocity and turbulent intensity at the nozzle exit (Re = 2000).

The jet was formed by ejecting air from the round nozzle into still air. The Reynolds number of the jet was defined by the velocity at the center of the nozzle exit U_{c0} and the diameter of the nozzle exit diameter D_0. The Reynolds number was set to 2000, where U_{c0} is 2.55 m/s. The frequency of the sinusoidal wave input to the loudspeakers, namely the frequency of the synthetic jets f_s, was set to 120 Hz (dimensionless frequency $St = f_s D_0/U_{c0} = 0.56$), which is the frequency of vortex ring formation in the natural transition. The input voltages of the sinusoidal wave E were set to 0.5, 1.0, and 2.0 V in amplitude. The three synthetic jets were driven sequentially with a phase difference of $2\pi/3$ rad. The driving frequency at this time, called the rotational frequency f_r here, was 120 Hz, identical to f_s.

Velocity profiles were measured with a hot-wire anemometer using an I-type probe on a line connecting the side with and without the synthetic jet. The measurements were performed 1 mm downstream from the nozzle exit, with the input voltage for the synthetic jets E as a parameter. The measured values are shown in Fig. 3, where r is the radial coordinate from the nozzle center. It is found that the mean velocity profiles do not change with or without the synthetic jet. The turbulence intensities are higher at the side with the synthetic jet for except of the case where E = 0.5 V.

3. Numerical Simulation

As shown Fig. 4, the nozzle shown in Fig. 1 was approximated as a cylindrical shape. Moreover, the excitation holes were approximated as square ducts. An unsteady numerical simulation was performed using OpenFOAM. For details of the numerical simulation method, please refer to the reports by Tanaka and Muramatsu [6] and Kobayashi and Muramatsu [5]. The inlet of the cylindrical nozzle gave a top-hat velocity profile as defined in Eq. (1). The constants a and r_0 in Eq. (1) were determined by actual measurements using a hot-wire anemometer. For Re of the jet is 2000, the constants a and r_0 in Eq. (1) are 30 and 0.45, respectively. The U_{noise} was applied as a white noise in time and space, and the value is ±0.5% of the mainstream velocity U_c. The velocity in the two directions perpendicular to the main flow was assumed to be zero.

$$U = \frac{1}{2} U_c \left(1 + U_{noise}\right)\left[1 - \tanh\left\{a\left(\frac{r}{D_0} - r_0\right)\right\}\right] \tag{1}$$

In this simulation, the synthetic jets were given as pressure boundary conditions at the entrance of the excitation holes. A periodic pressure disturbance p expressed by Eq. (2).

$$p/\rho = A \sin\left(2\pi f_s t + \phi_i\right) \tag{2}$$

where ρ, A, t, and ϕ_i are the density, amplitude, time, and phase difference, respectively. The amplitude A was set to 1.5 (m/s)^2.

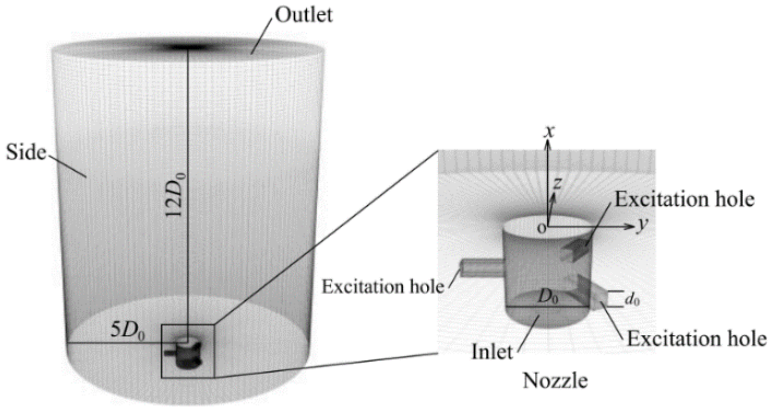

Fig. 4 Computational domain and a cylindrical nozzle with three excitation holes.

The results of the numerical simulation are shown in Figs. 5 to 7. Figure 5 illustrates the large-scale vortex structures extracted using the second invariant of the velocity gradient tensor, Q value. The yellow line in Fig. 5 indicates the position of the nozzle exit along the streamwise direction, and Fig. 5 reveals that a spiral structure is formed from the nozzle exit. Figures 6 and 7 show the azimuthal and radial velocity distributions at the positions indicated by the red lines in Fig. 5, x/D_0 = 2.00 (where the spiral structure is visible in the front) and 1.58 (where the spiral structure is at the back). Red and blue colors indicate positive and negative values, respectively, within a range of ±0.1 m/s.

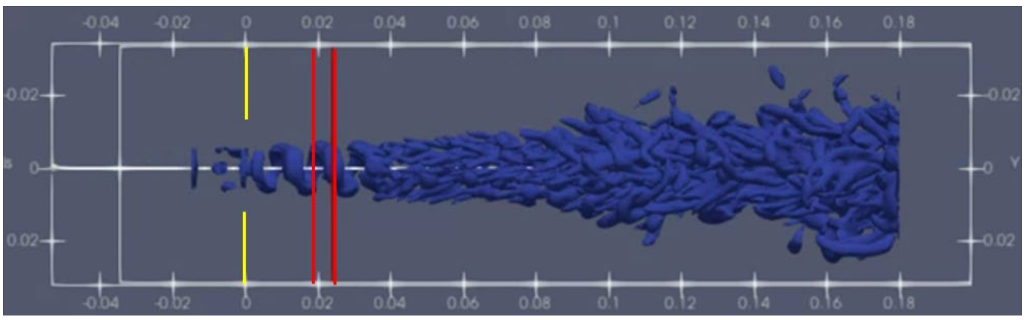

Fig. 5 Vortical structures of a controlled jet with three synthetic jets ($f_s = f_r$ = 120 Hz, Re = 2000).

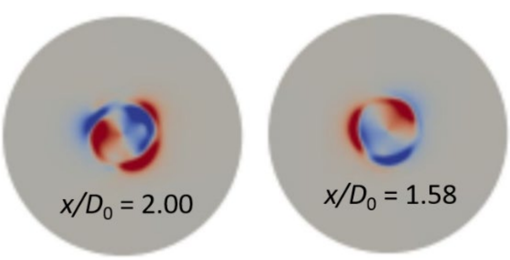

Fig. 6 Contours of azimuthal velocity at two sections in Fig. 5.

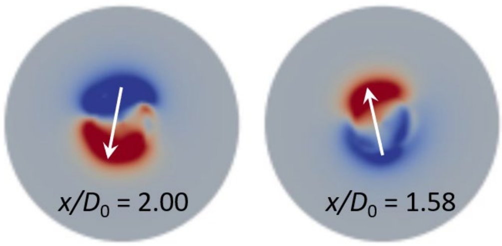

Fig. 7 Contours of radial velocity at two sections in Fig. 5.

4. Experimental Results

The cross section of the jets was visualized using a laser sheet of approximately 1 mm thick, after fine particles were introduced to the jet. Figure 8 shows visualized images of a cross section in the streamwise direction along the jet centerline. The distance x/D_0 represents the streamwise distance from the nozzle exit, dimensionless by the diameter of the nozzle exit D_0. For all input voltage E of 0.5 V, 1.0 V, and 2.0 V in this experiment, the vortex rings form at an oblique angle to the central axis of the jet. The jet column appears to meander due to the formation of oblique vortex rings. As E increases, the position at which the vortex ring forms and collapses moves upstream and the turbulence of the jet after the vortex ring collapses appears to become greater.

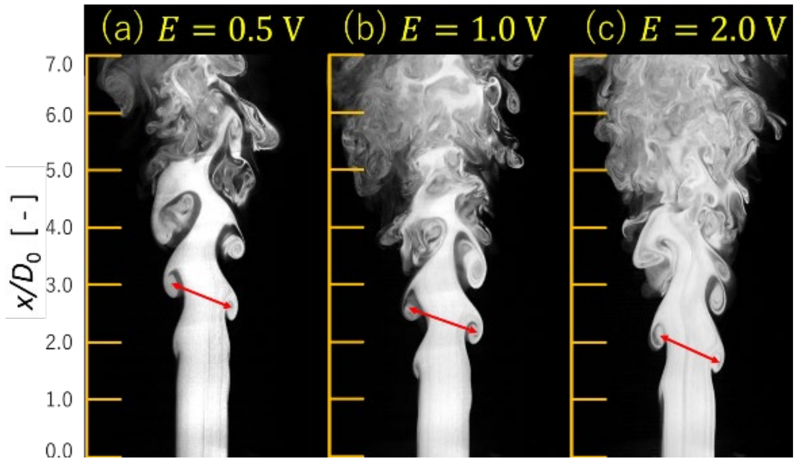

Fig. 8 Visualized images of streamwise cross-section on the jet centerline.

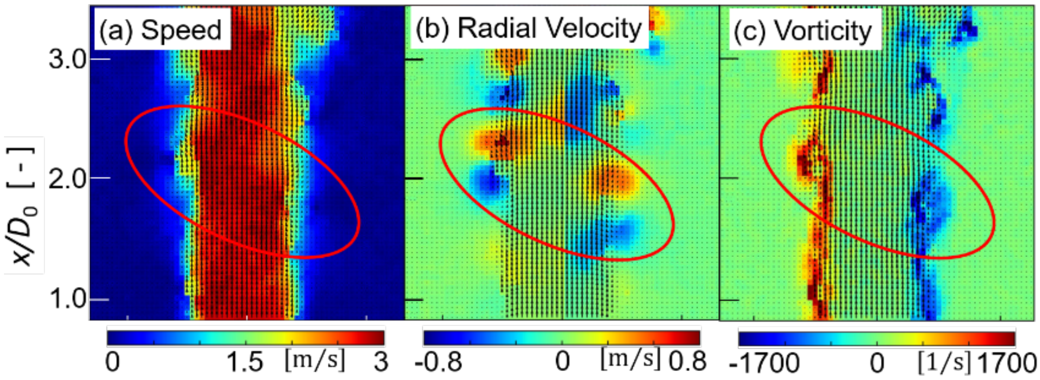

Fig. 9 Measured values on cross-section along the jet centerline using a PIV.

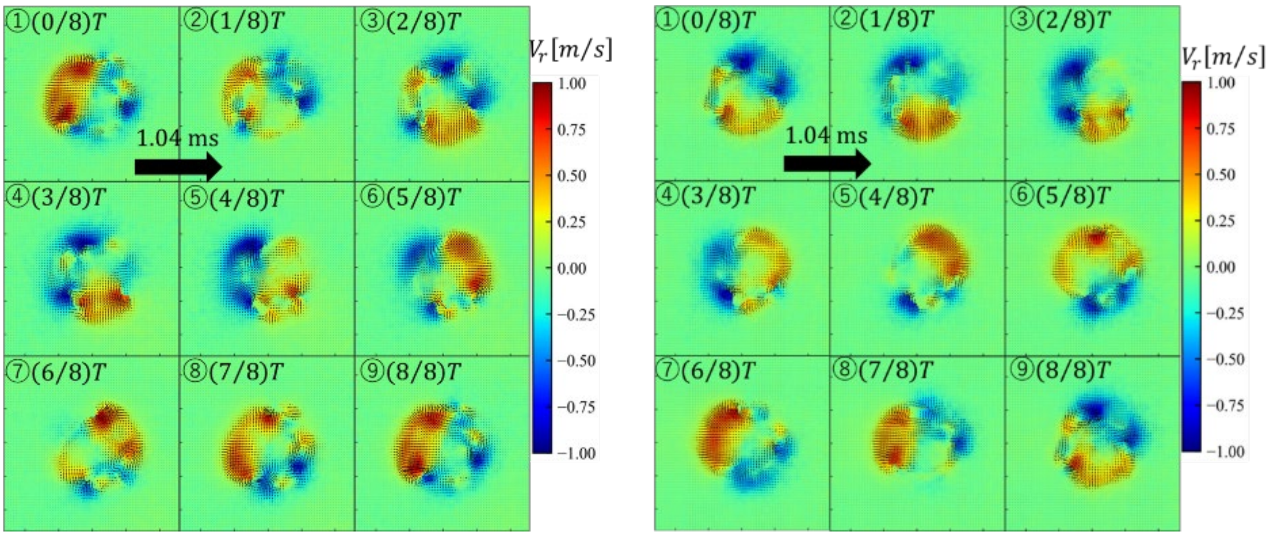

(a) $x/D_0 = 2.17$ (b) $x/D_0 = 2.00$

Fig. 10 Measured radial velocities on the horizontal cross-section using a PIV.

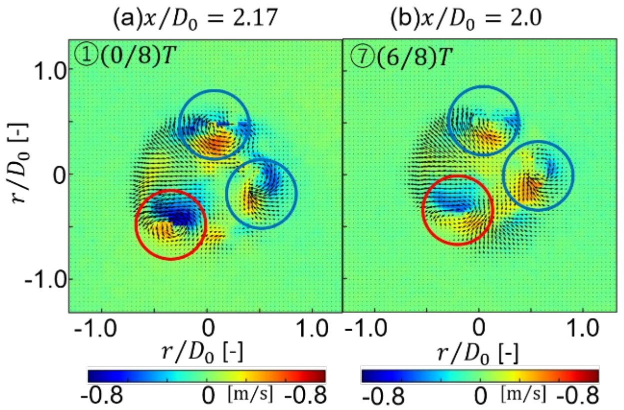

Fig. 11 Measured azimuthal velocities using a PIV.

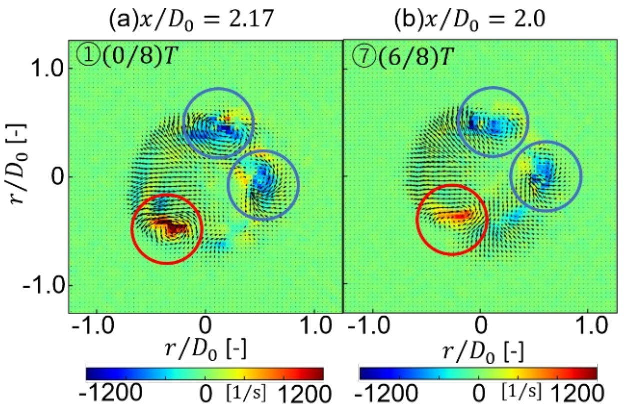

Fig. 12 Measured streamwise vorticities using a PIV.

Next, the results of PIV measurements for a jet with E of 1.0 V are shown in Figs. 9 to 12. In the PIV measurement, the jet was enclosed by a duct, fine particles were further mixed into the surrounding air, and the images were captured using a high-speed camera (Photron, SA-X2) at 12,500 fps. The image resolution was set to 1024 ×1024 pixels for both the streamwise and the orthogonal cross sections. The captured images were analyzed using an analysis software DynamicStudio (Dantec Dynamics) to determine the velocity and vorticity fields with an overlap of 50% and an interrogation area of 32 × 32 pixels. The captured image area was 32 mm × 32 mm in the main flow direction and in the horizontal direction.

Figure 9 shows the contour plots of (a) speed, (b) radial velocity, and (c) streamwise vorticity of the cross section along the central axis of the jet. In particular, the red-circled area highlights the tilted vortex ring. The radial velocity in Fig. 9 (b) is positive at the top of the vortex ring and negative at the bottom, illustrating the rotational nature of the vortex structure.

Figures 10(a) and (b) show the radial velocity at the cross sections of x/D_0 =2.17 and x/D_0 =2.0, respectively. The excitation frequency f_s (or rotation frequency f_r) was used to divide one period into eight parts for phase analysis. These cross sections are the regions where the vortex is predicted to form spirals based on observations from Figs. 8 and 9. The results align with the numerical simulation seen in Fig. 6. Since (1) in Fig. 10 (a) and (7) in Fig. 10 (b) are similar, we will compare the azimuthal velocity and streamwise vorticity for these phases. As shown in Fig. 7 and (1) and (5) in Fig. 10 (a), there exists a situation where the cross section is divided into two sections, one with positive and the other with negative velocity. Consequently, as indicated by the arrows in Fig. 7, there exists a state in which the flow is almost unidirectional within the plane. Compared with Fig. 5, it is found that a spiral vortex structure is formed on the flow direction side. Figure 11 and 12 display the contour plots of azimuthal velocity and streamwise vorticity, respectively. In both Figs. 6 and 11, the azimuthal velocity has regions of both positive and negative values in the azimuthal direction. The positive azimuthal velocities exit on the side toward the radial velocity. These figures show that when the radial velocity has a similar distribution, the azimuthal velocity and streamwise vorticity also have similar patterns, as indicated by the circles in the figures. In both figures, the red circles indicate regions of positive vorticity and the blue circles denote regions of negative vorticity. Two negative vorticity areas and one positive vorticity area are formed, forming an asymmetric flow structure.

5. Conclusion

It is demonstrated that a vortex with a spiral structure can be formed from the nozzle exit using synthetic jets. The radial velocity in the plane perpendicular to the main flow direction flows toward the side with the helical structure. The azimuthal velocity in this plane is not uniform, and has both positive and negative velocities. The flow structure in this plane is asymmetric.

References

[1] Bachelor, G. K. and Gill, A. E., "Analysis of the stability of axisymmetric jets", *Journal of Fluid Mechanics*, Vol. 14, No. 4 (1962), pp.529-551.

[2] Koch, C. R., Mungal, M. G., Reynolds, W. C., and Powell, J. D., "Helical modes in an acoustically excited round

air jet", Physics of Fluids A, Fluid Dynamics 1 (1989), p.1443.

[3] Kiwata, T., Usuzawa, T., Komatsu, N., Kimura, S. and Oshikai, P., "Flow structure of a coaxial jet with axisymmetric and helical instability modes", *Journal of Fluid Science and Technology*, Vol. 6, No. 4, (2011), pp 437-452.

[4] Tanaka, K. and Muramatsu, A., "Observation of Vortex Structures in a Round Jet with Artificially Branched Flows Using Time-Resolved 3D Imaging ang PIV", *Proc. The 31ST International Symposium on Transport Phenomena*, Online, ISTP31_paper_90, (2020), pp, 1-4.

[5] Kobayashi, Y. and Muramatsu, A., "The formation of helical mode in a round jet using synthetic jets", *Proc. The 7th International Conference on Jets, Wakes and Separated Flows,* Online, ICJWSF2022-E05, (2022), pp 1-6.

[6] Tanaka, K and Muramatsu, A., "Vortex structures in the near field of a round jet with controlled side jets", *Proc. 32th CFD Symposium,* Online, A10-3, (2020), pp 1-4, (in Japanese).